Solving simultaneously for acquisition perturbations in a deep-water node survey in Santos Basin, Brazil

Marilia Carneiro, Pedro Barros, Marcela Ortin, Claudio Bagaini, Paal Kristiansen, Bernardo Quijano, SLB

This paper was prepared for presentation during the 18th International Congress of the Brazilian Geophysical Society held in Rio de Janeiro, Brazil, 16-19 October 2023.

Abstract

We present a successful case study of estimating and correcting for acquisition-related perturbations in a deep-water ocean-bottom node acquisition. The method uses the picked and modeled direct arrival, in conjunction with the first-order water-bottom multiple, to simultaneously invert for water velocity variation, clock drift, node and source position corrections. This approach reduces the correlation between the estimated clock-drift and node depth. It also incorporates two different water velocity logging tools, the pressure inverted echo sounders and sound velocity profiles, which are used to compute the depth-dependent reference water velocity and to estimate the temporal variations of the water velocity.

Introduction

The quality of ocean-bottom node (OBN) data acquired in deep water can be affected by several acquisition-related perturbations, such as uncertainties in node and source positions, temporal variations of the temperature and salinity of the water layer that affect the water velocity, and additionally clock-drift, due to variable clock aging or loss of information synchronization between deployment and recovery. These perturbations must be addressed to avoid errors in the imaging process and allow for the realization of the full potential of the data.

The inaccuracies in positioning and variations in water velocity estimation can significantly affect the data quality. Attempts have been made to estimate and correct for these deviations. Studies made by Olofsson (2010) showed that the impact of typical errors in clock-drift, node and source positions, and temporal variations of water velocity of less than 0.5 m/s, leads to travel time errors larger than 1 ms. Docherty (2012) concluded that a successive estimation of positioning and water variations leads to ambiguities in the solution and is time consuming. Amini (2016) proposed to jointly estimate node position and water velocity from direct arrivals, but without considering the clock-drift and source position.

To mitigate the effect of these perturbations, we developed a novel inversion approach, that simultaneously estimates the correction for all the aforementioned uncertainties (Mujizert 2021 and Seymour 2021). This method is an extension of the method proposed by Oshida A. (2008), and estimates simultaneously four perturbations: node and source positions, clock-drift, and temporal variations of the water velocity. In addition to the direct arrival (DA), the present approach optionally incorporates the first-order water-bottom multiple (WBM), as an extra constraint, to reduce the clock-drift and node depth crosstalk.

This workflow also comprises water velocity measurements, from two different logging tools, the pressure inverted echo sounders (PIES) and sound velocity profiles (SVP), as complementary information for water velocity variation estimation, as proposed by Wang, et al., 2012. Bagaini (2021) has shown the value of using these complementary measurements. The PIES record the average sound velocity through the water column from the seabed to the sea surface over time. SVPs measure the sound velocity as a function of the water depth at a specific time. Both measurements are limited to a restricted number of locations.

In this study of a deep-water 3D OBN survey, the difference between observed and predicted DA and WBM were used to simultaneously invert for four perturbation types. Additional measurements of water layer from PIES and SVPs were used to derive the reference water velocity.

Method

Acquisition perturbations, such as node and source positionings, clock-drift, and temporal variations in water velocity are manifested as an error between the picked and predicted direct arrival times.

The simultaneous acquisition perturbation correction is a linearized inversion, pursuing to minimizing the difference of the modeled and picked direct arrival travel times, described as:

$$\sum_{sr}[\boldsymbol{T_d} - \boldsymbol{T_{sr}}] \approx \sum_{sr}^{i} \frac{\boldsymbol{\partial T_{sr}}}{\boldsymbol{\partial m_i}} \boldsymbol{dm_i} \qquad (1)$$

where T_{sr} is the travel time between source and receiver locations, respectively (x_s, y_s, z_s) and (x_r, y_r, z_r), and m_i is the variation model parameters, with $dm_{ir} = \left[dx_r, dy_r, dz_r, c_{0_r}, c_{1_r}, c_{2_r}, dx_s, dy_s, dz_s, dv_r\right]^T$, being c_r the model clock-drift. In this way, the inversion computes the correction for node, source, clock drift, and velocity. The inversion is further extended to incorporate the first order multiples as an extra constraint to reduce the clock-drift and node position correlation.

Case study

This OBN seismic survey is situated in the Santos basin, offshore Brazil, in an area of approximately 2 km of water depth. The acquisition was conducted over an area of ~1,000 km^2 and utilized 3,000 nodes.

The inversion requires the predicted DA and WBM events, the respective picks, and a depth variant reference water velocity to estimate the corrections. The reference velocity will be also used in the earth model for imaging.

With the purpose of modeling the DA and WBM accurately for the inversion, it is crucial to study the water layer. The propagation of the direct wave is dependent on the velocity variations in the water column. Therefore, to guide and validate the simultaneous inversion corrections, the analysis is complemented with direct measurements of the water velocity.

The analysis of the water column was made using the additional data provided by PIES and SVPs, which are types of sensor-logging devices, used for the direct measurements of the speed of sound in the ocean.

The PIES sensors measure the average sound velocity through the water column, from the seabed to the sea surface and are deployed at the water bottom for the duration of the survey or until the nodes in their vicinity are recovered. SVPs measure the sound velocity as a function of the water depth at a limited number of locations and are attached to the remotely operated vehicles (ROVs), used to deploy the nodes, and record the variation through the water column while the nodes are deployed and retrieved.

PIES and SVPs data were recorded during this acquisition and, therefore, used to estimate the water velocity function profile. The water velocity variation is estimated from a combination of pressure measurements from the PIES and calibrated with the SVP measurements and the tidal fluctuations. Figure 1 (left) shows the relation of average velocity measured by PIES and SVP at their respective locations along the acquisition days, obtained by joint processing. Figure 1 (right) shows the 5th order polynomial fitted to the selected measured SVP profiles. The resulting polynomial function is to be used to model the DA and WBM timing for the different source receiver pairs, and moreover for the velocity model building.

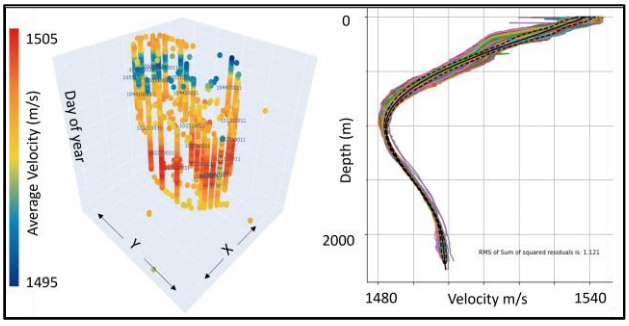

Figure 1: (Left) water velocity average measured by PIES and SVP at their respective XY locations against the acquisition days. The color represents the average velocity. (Right) Selected sound velocity profiles with 5th order polynomial fitted.

With the aim of enhancing the DA and WBM picking, a data conditioning workflow was applied to the hydrophone component P (immediately after reformat stage), which the impact is shown in Figure 2. This data conditioning included offset limitation, tidal statics (that can be estimated from PIES measurement), source directivity compensation based on source modeling, preliminary debubble, zero-phasing, high-cut filtering, linear clock-drift correction, and geometric spreading.

The iterative high-resolution picking, with offset limitation, is made for direct arrival and water bottom multiple, as represented in Figure 3.

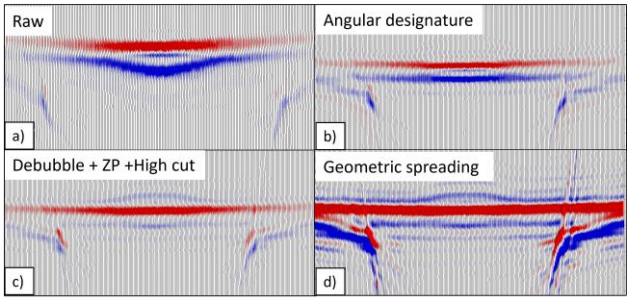

Figure 2: Flatten DA for a single node for a) the raw data, b) after angular designature, c) after debubble, zero-phasing, and high-cut filtering, d) after geometric spreading.

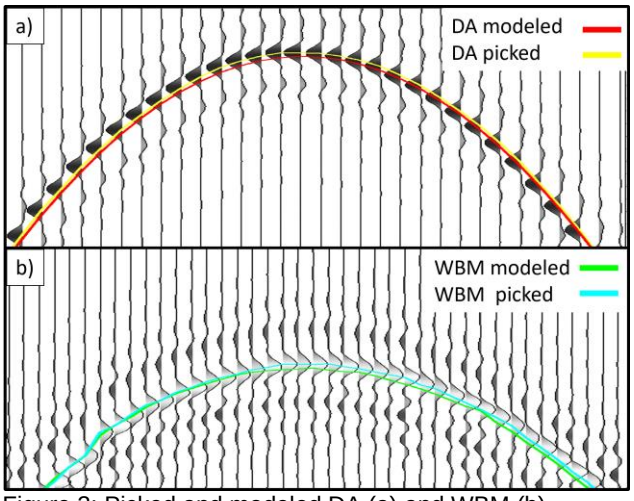

Figure 3: Picked and modeled DA (a) and WBM (b).

With this information, the inversion simultaneously estimates the corrections, and these corrections are later applied to the data in time domain.

Inversion results are analyzed in different domains. The residual travel time, determined by the difference between predicted and picked direct arrival, is the first QC to be evaluated. In Figure 4 we show the residual travel times input (a) and after the clock-drift, node position, water velocity and source position corrections are applied (b). Each circle in the graphs represents a node and the colors represent the residual travel time for each source in a 2500-m radius around the node. As expected, the residuals decrease after applying the simultaneously derived corrections. Figure 5 shows a DA closeup for a single node after moveout correction with water velocity. The jitter, highlighted by the red arrows in panel a), is reduced after the application of the estimated corrections, as indicated by the green arrows in panel b).

In Figure 6 the reference water velocity function derived from SVP is observed in black, while the cloud of values represents the inverted water velocity for each shot, used to estimate the water velocity time-shift correction plotted in a red-white-blue color scale.

An evaluation of the average velocities inverted from direct arrivals and the measured PIES, along the days of the acquisition is displayed in the Figure 7. Each of the colored dots represent the measured PIES velocities and each of the black dots represents the velocities estimated by the inversion. A good matching between the estimated velocities and the measured PIES is observed.

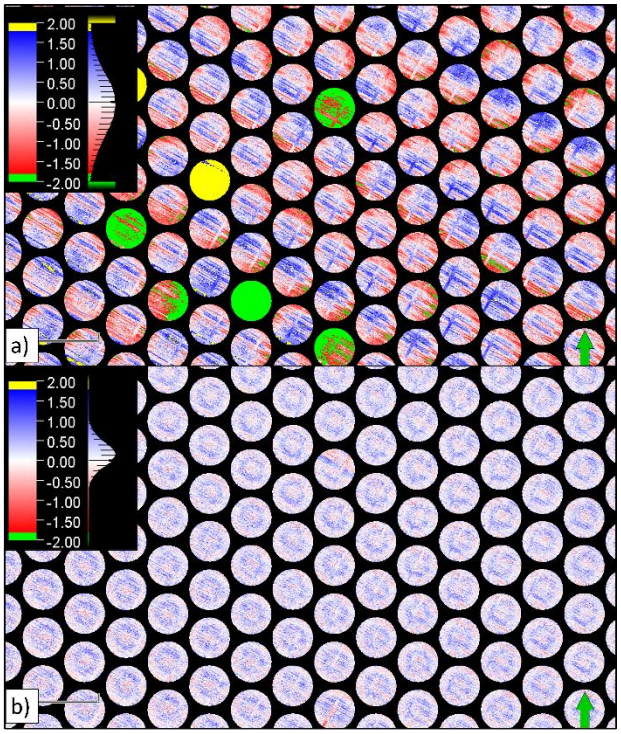

Figure 4: Travel time residuals map at node position. Each circle in the graphs represents a node and the color the residual travel time for each source in a 2500-m radius around the node: a) input, b) after apply clock-drift, node positioning, water velocity, and source position corrections.

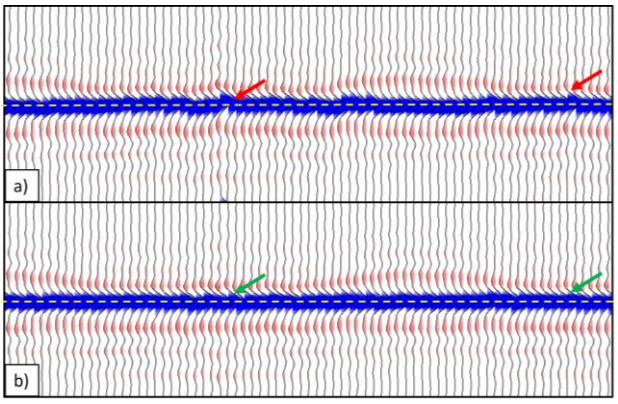

Figure 5: DA receiver node flattened with water velocity. Before (a) and after (b) application of estimated corrections.

A high-resolution water bottom depth survey was acquired in the area previously. To validate the estimated correction results in the image domain, the interpretation of the water bottom in a Kirchhoff prestack depth migration (KDM) was used. Just the first 2000-m offset of the full-azimuth P-only data was used, and the first-order multiple was migrated as primary, mimicking a downgoing wavefield using only the hydrophone information. For the water velocity the function derived from the SVPs by a fifth order polynomial was used.

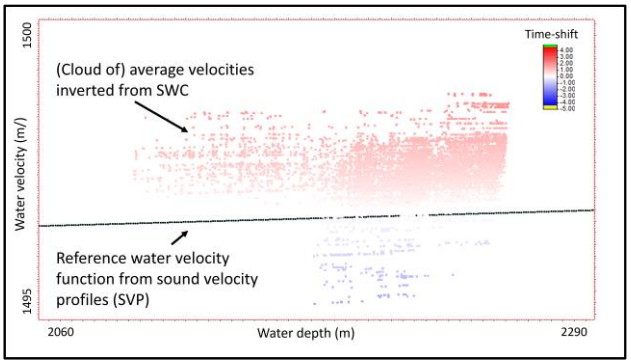

Figure 6: In black reference water velocity derived from SVP measurement. Dots represent the average velocity estimated by the simultaneous inversion for each shot and the color represent the estimate time shift to be applied as correction.

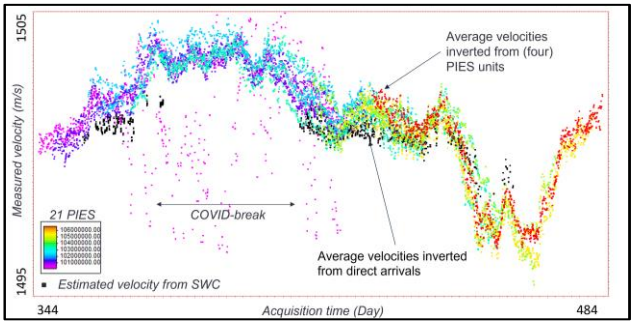

Figure 7: Average water velocity acquisition inverted from direct arrivals. Each colored dot represents PIES velocities, and each black dot represents the velocities estimated by the inversion.

In Figure 8 the water bottom interpreted on the KDM image with (a) and without (b) corrections applied. In both pictures the black dashed line represents the high-resolution bathymetry. A closer match between the picked water bottom and the trusted high-resolution bathymetry horizon is observed once the inversion results are applied.

Figure 9 shows an area QC of the differences between bathymetry and the interpreted water bottom horizon, without (a) and in (b) with corrections applied. The histograms extracted from the maps show how the difference between surfaces, after the perturbations were corrected, is smaller and zero centered.

After imaging, residual moveout at the water bottom is QCed. The moveout is affected by temporal variations in the water velocity, misposition of nodes and sources and any timing errors, like the ones related to clock drift. The RMS gamma map in Figure 10 shows the residual moveout at water bottom. In (a) strips in the source direction due to changes in water velocity are visible as is the imprint of two nodes with nonlinear clock drift. In (b) those effects have been minimized as the general residual moveout after the derived corrections were applied.

Conclusions

The simultaneous inversion for water velocity, source and receiver positioning, and clock drift applied in this deep water OBN survey in Santos basin Brazil compensates for the main acquisition perturbations that deep water nodes suffer from. The use of the first-order water-bottom multiple in conjunction with the direct arrival minimizes the crosstalk between the clock drift and node depth corrections.
Different QCs in time and image domain, as well as the matching between the inverted water velocity profile in time with the independent PIES measurement, validate the quality of the derived corrections. The time domain QCs exhibit a good matching between the modelled and predicted direct arrival. While in the image domain, the significant reduction of the residual moveout, observed in the water-bottom event in the migrated gathers after the correction and the close matching between the interpreted water bottom in the near-offset full-azimuth KDM with the water bottom depth from high-resolution bathymetry survey, reassures the value of these results.

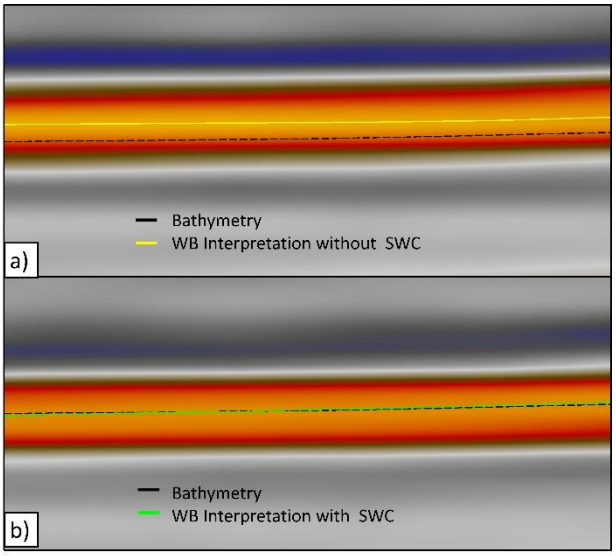

Figure 8: Water bottom horizon from the KDM. The black dashed line represents the high-resolution bathymetry. In a) we show the migrated water bottom obtained without applying corrections to the input data for the migration, and the respective picked water bottom horizon is shown in yellow. In b) we show the data migrated after corrections have been applied, and the interpreted water bottom horizon is shown in green. In the non-corrected data, the difference between high-resolution bathymetry and picked water bottom is in the order of 2.5 meters while in the corrected data the difference is negligible and related to the difference in the resolution of the two measurements.

Acknowledgments

We thank SLB for the permission to publish this work and Petrobras, Shell and Petrogal for the authorization to use the data shown in this abstract.

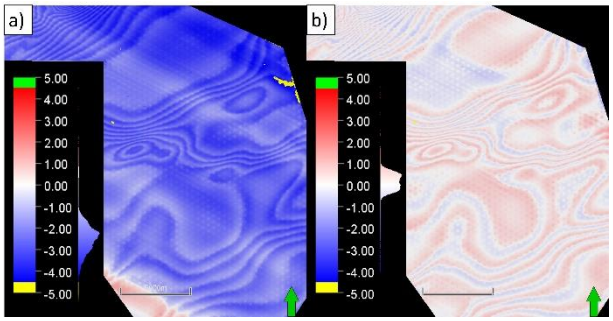

Figure 9: Difference map between bathymetry and the WB picked horizons. In a) is without application of estimated corrections and in b) is with.

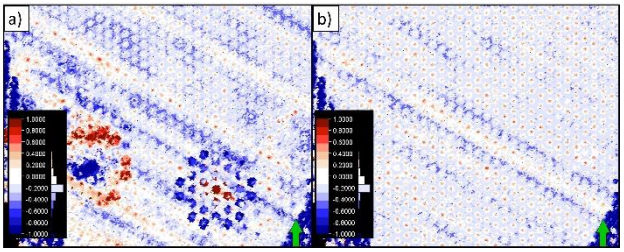

Figure 10: RMS map picked in the CIP gathers. In a) is without application of estimated corrections and in b) is with.

References

AMINI A., PENG, H., ZHANG, Z., HUANG, R., YANG, J., N. 2016. Joint inversion of water velocity and node position for ocean-bottom node data. *In:* SEG, Expanded Abstracts, 5490-5494.

BAGAINI, C., MUJIZERT, E., KAPLLANI, K., SEYMOUR, N. [2021] On the usage of direct measurements of water velocity in deep water OBN surveys. *In:* SEG First International Meeting for Applied Geoscience & Energy Expanded Abstracts

DOCHERTY P., AND HAYS, D., N. 2012. Ambiguities in direct arrival time inversion of ocean bottom nodes. *In:* EAGE Conference & Exibition, Extended Abstracts.
MUJIZERT, E., BAGAINI, C., KAPLLANI, K., SEYMOUR, N. [2021] Simultaneous estimation of water velocity, node position, and clock-drift for ocean bottom node data.

SEYMOUR, N., BAGAINI, C., MUYZERT, E., KAPLLAN, K., AND SALGADOE, M., N. 2021. Sparse OBN image improvements by correction for acquisition errors. *In:* SEG Technical Expanded Abstracts: 81-85.

OLOFSSON B. AND WOJE, G., N. 2010. Ensuring correct clock timing in ocean bottom node acquisition. *In:* SEG Expanded Abstracts.

OSHIDA A. KUBOTA R., NISHIYAMA E., ANDO J., KASAHARA J., NISHIZAWA A, & KANEDA K. N., 2008. A new method for determining OBS positions for crustal structure studies, using airgun shots and precise

bathymetric data. Exploration Geophysics, 39:1. - 2008. - pp. 15-25.

WANG, K., P.; HATCHELL, C.; UDENGAARD, K.; CRAFT, K.; DUNN, S. 2012, Direct Measurement of Water Velocity and Tidal Variations in Marine Seismic Acquisition. *In:* SEG Expanded Abstracts, 1-5.